

---

# 3D Spectroscopy of Wind Driven Nebulae: The Large Western Knot in the Halo of NGC 6543

David Martín-Gordón<sup>1</sup>, José M. Vílchez<sup>1</sup>, Angels Riera<sup>2,3</sup>, and Sebastián Sánchez<sup>4</sup>

<sup>1</sup> Instituto de Astrofísica de Andalucía, CSIC. Apdo. 3004, 18080 Granada - Spain. [dmg@iaa.es](mailto:dmg@iaa.es), [jvm@iaa.es](mailto:jvm@iaa.es)

<sup>2</sup> Departament de Física i Enginyeria Nuclear, Universitat Politècnica de Catalunya, Vilanova i la Geltrú - Spain. [angels.riera@upc.es](mailto:angels.riera@upc.es)

<sup>3</sup> Department d' Astronomia i Meteorologia, Universitat de Barcelona, Barcelona - Spain.

<sup>4</sup> Calar Alto Observatory Centro Astronómico Hispano Alemán, 04004 Almería - Spain. [sanchez@caha.es](mailto:sanchez@caha.es)

**Summary.** The history of stellar mass loss of massive and intermediate mass stars is written in their wind driven-nebulae. Fast winds can provide an extra source of heating for the thermal balance of the haloes of PNe and WR nebulae. The comparison of the emission of different states of ionization or different emission conditions provides a direct evidence for finescale structure within the halo of the nebula. In this work we present new results of 3D spectroscopy taken with the PMAS/PPAK Instrument for the halo of the nebula NGC 6543. The large Western Knot in the halo of this young planetary nebula is an excellent place to derive new spectroscopic constraints in order to evaluate the role of photo-ionization as the main excitation mechanism.

**Key words:** Nebulae: planetary nebulae – Nebulae: photoionization – Nebulae: shock excitation – Nebulae: 3D spectroscopy

## 1 Introduction

The history of stellar mass loss is written in the extended wind-driven nebulae around massive (WRN) and intermediate mass stars (PNe). Fast winds can produce shock excitation of the interstellar medium in the haloes of PNe and WR nebulae providing an extra source of heating for their thermal balance. We are performing an observational program aimed to evaluate the realistic impact on the interstellar medium of these effects. A search for possible footprints of shock-heated gas in the extended haloes of wind-driven nebulae has been carried out using deep multi-filter imaging of a sample of WR and PNe nebulae. The comparison of the emission of different states of ionization or different emission conditions provides a direct evidence for fine-scale structure within the halo of the nebula. Subsequently, 3D spectroscopy has been performed for several locations of the nebulae which are

candidate to host an extra heating contribution as indicated by our previous 2D ionization structure maps.

### 1.1 The Extended Halo of the NGC 6543 Nebula

The outer haloes are of great interest as they are presumably the remains of the original stages of mass loss from the progenitor stars. While WR Ring nebulae typically show a wind-blown bubble of interstellar material, planetary nebula can show extended ionized halo; NGC 6543 is a typical example of a well known PN halo [1, 2]. Here we do not present a study of the central parts of this well known nebula, but we are interested in the ionization of selected faint (filamentary) structures and knots detected in its outer halo. It has been claimed that the haloes of some multiple shell PNe, and in particular in the case of NGC 6543, could be much hotter than their respective core nebulae [2, 4, 5, 6]. As shown in [5] that photoelectric heating is not able to reproduce the high electron temperatures observed in the halo of NGC 6543, claiming that an extra heating source would be required. A candidate for this extra energy source is the fast wind passing the cold filamentary knots observed in the haloes of this PN. In our previous work [3] we have shown how the ionization structure of [OII]/[OIII] across the global nebula seems to follow the locus expected for models of type II PNe and HII regions. The predictions of the shock models used do not appear to match the major part of the observations. However, a substantial part of the observed [SII] emission, a good tracer of the low ionization species, occupies an area of the diagnostic diagram which is out of the locus of the predictions for PN models. It is striking how this handful of points of the halo may show values showing a (real) measurable difference respect to the rest of the points. This suggestion of our previous work needed a spectroscopic confirmation. In this work we present deep 3D spectroscopy of the Western Halo Knot (WHK) of this nebula aiming to provide further constraints for the thermal balance of the halo gas.

### 1.2 Diffuse Gas Surrounding the Western Halo Knot

Recently [7] have studied the kinematics of the large WHK of NGC 6543. They have concluded that there exist gas flows around the, otherwise kinematically inert, knot. This gas is observed to be developing velocities comparable to the sound speed as the gas is photo-evaporated off the ionized surface. These authors find no evidence for the WHK being interacting with a fast wind, and they suggest that this knot structure was not a product of instabilities in the interface between the fast and the asymptotic giant branch winds. A scenario was proposed in which the WHK is embedded in a slowly expanding red giant wind whereas its surface is photo-ionized by the central PNe star. We have detected spectroscopically the possible counterpart of this gaseous component as shown in Fig. 1, thus discriminating the physical properties of the brighter sub-knots structure across the knot with respect to this low surface brightness gaseous envelope.

## 2 Preliminary Results

In this work, as an example, we present new results of 3D spectroscopy taken with the PMAS/PPAK Instrument (Calar Alto Observatory, Spain) for the halo of the

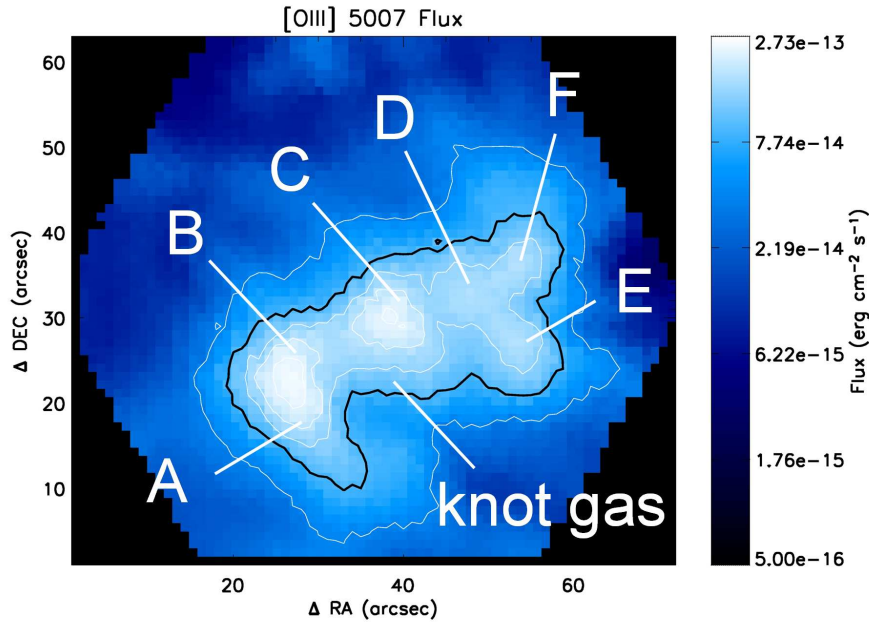


**Fig. 1.** This map shows the flux of the 5007 [OIII] line in units of  $\text{erg cm}^{-2} \text{s}^{-1}$ . The solid lines delineates the isocontour corresponding to  $4.5 \times 10^{-14}$ ,  $1 \times 10^{-13}$ ,  $1.5 \times 10^{-13}$ ,  $2 \times 10^{-13}$  and  $2.5 \times 10^{-13}$  flux. The sub-knots marked on the map as well as the boundary of the knot gas (black solid line) refers to the same features identified in [7]. North is down and West is right. Figures 2 and 3 have the same orientation.

nebula NGC 6543. The large Western Knot in the halo of this young planetary nebula is an excellent place to derive new spectroscopic constrain in order to evaluate the role of photo-ionization as the main excitation mechanism. PPAK is a 3D spectrograph with 330 densely packed optical fibers with a nominal spatial sampling of 2.7 arcseconds. A total of three pointings ( $\times 3$  exposures each) per field were taken following a dithering technique, in order to attain a spatial sampling of 1 arcsec. The spectral dispersion of the data is  $0.3 \text{ \AA}/\text{pixel}$  in high resolution, and  $1.6 \text{ \AA}/\text{pixel}$  at intermediate resolution and the field covered by the data is of  $1 \text{ arcmin}$  in diameter. All the maps have been obtained measuring the flux of the selected emission line in the whole 990 spectra of each datacube. An automated procedure has been designed to perform flux measurements, including continuum subtraction and error calculation.

#### *Electron Temperature*

Electron temperature ( $T_e$ ) were calculated using the [OIII]4363/(4959+5007) line ratio. Figure 2 shows a substantial variation in ( $T_{e[\text{OIII}]}$ ) across the WHK.  $T_{e[\text{OIII}]}$  values tend to be lower ( $\sim 1.4 \times 10^4 \text{ K}$ ) in the brighter sub-knots, along the WHK, though some slight shifts between both [OIII] flux and  $T_{e[\text{OIII}]}$  extrema are notice-

able. On the other hand, the tenuous gas embedding the knots (the knot gas shown in Fig. 1) appears much hotter, reaching values of order  $\sim 2 \times 10^4$  K. The error of the temperature map was calculated from the signal/noise ratio obtained for each individual [OIII] line flux measurement.

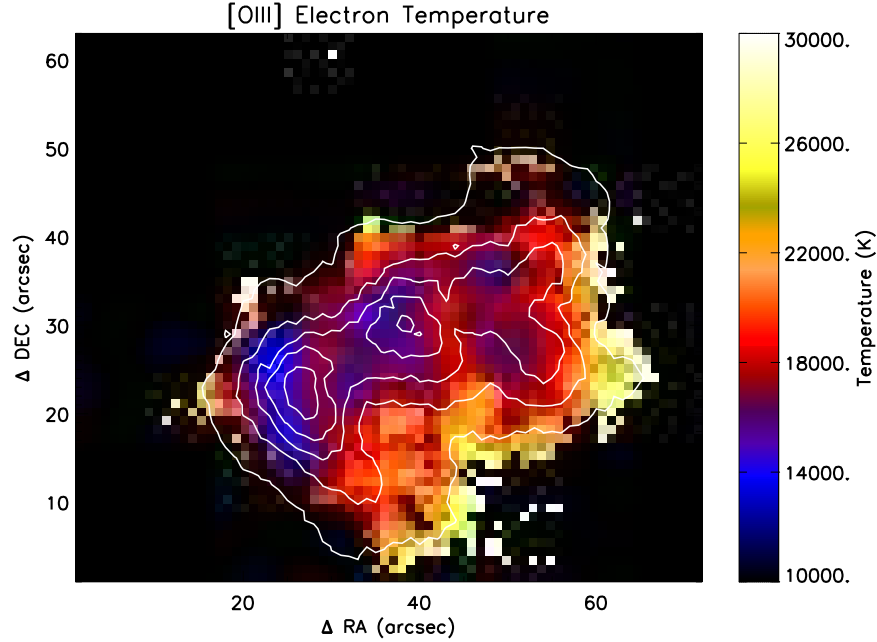


**Fig. 2.** The electron temperature,  $T_{e[\text{OIII}]}$ , map derived from the ratio of the collisionally excited lines [OIII]4363/(4959+5007).

### *Electron Density*

The electron density values (Fig. 3 left) derived range from the low density limit up to  $\sim 600 \text{ cm}^{-3}$  though some degree of structure is apparent; interestingly enough the higher density zones do not follow the knots structure seen in the [OIII] flux in Fig. 1; however, this density map appears to show a much closer relation with the electron temperature distribution.

### *Main Results*

A gaseous envelope around the WHK of NGC 6543 has been detected and measured using 3D spectroscopy (Fig. 1). Density values range from the low density limit up to  $\sim 600 \text{ cm}^{-3}$  (Fig. 3 left). Electron temperature shows conspicuous variations, with values going from 1 to  $2.5 \times 10^4$  K. The values of the electron temperature in the [OIII] zone present a mean  $T_{e[\text{OIII}]} = 1.91 \times 10^4$  K, a mode  $T_{e[\text{OIII}]} = 1.65 \times 10^4$  K and a standard deviation of  $0.35 \times 10^4$  K. The diffuse gaseous envelope appears to

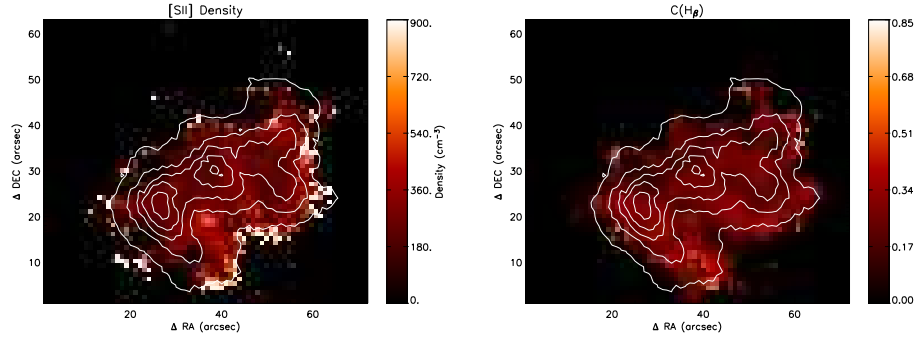


**Fig. 3.** **Left:** Map of the density of the WHK of NGC 6543, in the single ionized zone, obtained from the [SII]6717/6731 ratio. **Right:** Map of the reddening coefficient,  $C(H_\beta)$ , of the WHK of NGC 6543 derived from the  $H_\alpha/H_\beta$  ratio assuming case B recombination for low density ( $< 1000 \text{ cm}^{-3}$ ) and an average electron temperature of  $1.5 \times 10^4 \text{ K}$ .

be hotter and denser than the gas of the sub-knots (Fig. 2). The average reddening is low, presenting a smooth spatial distribution but with some degree of small scale structure (Fig. 3 right).

## References

1. Luridiana, V.; Pérez, E.; Cerviño, M.: 2003, AJ 125, 3196
2. Manchado, A.; Pottasch, S.R.: 1989, A&A 222, 219
3. Martín-Gordón, D.; Vílchez, J. M.; Riera, A.: 2005, Memorie della Società Astronomica Italiana, 76, 488
4. Meaburn, J.; Nicholson, R.; Bryce, M.; Dyson, J. E.; Walsh, J. R.: 1991, MNRAS 252, 535
5. Middlemass, D.; Clegg, R. E. S.; Walsh, J. R.: 1989, MNRAS 239, 1
6. Middlemass, D.; Clegg, R. E. S.; Walsh, J. R.; Harrington, J. P.: 1991, MNRAS 251, 284
7. Mitchell, D.L.; Bryce, M.; Meaburn, J., et al: 2005, MNRAS 362, 1286